PHYSICAL REVIEW B **78**, 140507(R) (2008)

Mapping the superconducting condensate surrounding a vortex in superconducting V_3Si using a superconducting MgB_2 tip in a scanning tunneling microscope

N. Bergeal, Y. Noat,* T. Cren, Th. Proslier, V. Dubost, F. Debontridder, A. Zimmers, and D. Roditchev
Institut des Nanosciences de Paris, CNRS UMR 7588, Campus Boucicaut, 140 Rue de Lourmel, F-75015 Paris, France

W. Sacks
Institut de Mineralogie et de Physique des Milieux Condensés, CNRS UMR 7590, Campus Boucicaut, 140 Rue de Lourmel, F-75015 Paris, France

J. Marcus
Institut Néel, CNRS/UJF, B.P. 166, 38042 Grenoble Cedex 9, France

(Received 9 October 2007; revised manuscript received 3 September 2008; published 8 October 2008)

As shown recently [Proslier *et al.*, Europhys. Lett. **73**, 962 (2006)], it is possible to map the superconducting (SC) condensate by measuring locally the Josephson tunneling current. We apply this technique to image the vortex lattice in V_3Si which is used as the simplest example of a spatially varying quantum condensate. The Josephson scanning tunneling microscope (JSTM) maps revealed the vortex lattice with the Josephson effect being present outside the vortices and disappearing progressively toward the vortex core. The characteristic length scales of a vortex observed in the Josephson regime are compared to the ones obtained in the quasiparticle regime. We demonstrate that the JSTM allows a nanometer scale resolution of the SC condensate that may be applied to inhomogeneous phases such as high-T_c superconductors.

DOI: 10.1103/PhysRevB.78.140507 PACS number(s): 74.25.Ha, 74.72.Jt, 75.30.Fv, 75.40.−s

Scanning tunneling microscopy (STM) and spectroscopy (STS) have been key techniques to probe the superconducting (SC) state on a nanometer scale. Applied to conventional superconductors, STM has allowed, among numerous examples, the study of the vortex lattice.[1] In high-T_c superconductors, it revealed (i) a nanometer variation in the SC gap and (ii) the presence of pseudogap regions above and below the SC transition temperature.[2] One hypothesis explaining the pseudogap is the existence of noncondensed Cooper pairs in these regions.[3] Unfortunately, STS probes the SC condensate indirectly through the quasiparticle (QP) excitations of the SC condensate, and thus is not a proof of the existence of coherent Cooper pairs.

A straightforward manner to probe the SC condensate directly would be to measure locally the Josephson current (JC) between a surface and a tip, both superconducting.[4] Indeed, if the barrier is sufficiently narrow, the overlap between macroscopic SC wave functions of the tip and the sample may result in a measurable current of Cooper pairs.[5] The JC is therefore a direct consequence of the existence of SC condensates in both tunneling electrodes. The relevant energy scale governing the pair tunneling is the Josephson energy E_J. At zero temperature, for identical tip and sample superconductors, the Josephson coupling energy is $E_J = \frac{\pi\hbar\Delta}{2e^2R_N}$, where R_N is the tunneling resistance in the normal state and Δ is the SC gap. Such a local JC was first observed on Pb film and $NbSe_2$ crystal using Ag-Pb tips by Dynes *et al.*[6] Later, a detailed analysis of SC-SC local tunneling junctions was done by Rodrigo *et al.*[7] In the former experiments,[6] the thermal energy was comparable to E_J and the current was well described by the model of Ivanchenko *et al.*[8] for the JC in the fluctuation regime. Finally, the first spatial JC maps on inhomogeneous SC thin films of MgB_2 were realized.[9]

In this Rapid Communication we present a JSTM of vortices in the conventional superconductor V_3Si. We first prove the existence of a JC by measuring its dependence on the tip-sample distance. In the second part, we demonstrate that the Josephson effect diminishes progressively toward the vortex core over the scale of ~5–10 nm and becomes zero inside it, concording with the vanishing of the SC order parameter. While this result might appear somewhat trivial in the case of a conventional SC, it represents an important step before achieving JSTM in nonconventional superconductors.

The SC tips were made using freshly cut Pt/Ir wires with MgB_2 grains glued on their extremity with silver epoxy.[10] The SC tips were hence constituted by a small MgB_2 grain with unknown orientation. One may expect two contributions to the density of states of such a MgB_2 tip in the SC state: the main one from the three-dimensional (3D) π band, with its characteristic SC gap of 2–3 meV, and a smaller one from the two-dimensional σ band, with a gap of about 7 meV.[10,11]

V_3Si appears to be a good candidate for Josephson scanning tunneling microscopy. Indeed, as a member of the A15 family,[12] it has one of the highest T_c (17.1 K) among the conventional superconductors and hence has one of the largest SC gaps ~2.4–2.8 meV.[13] The bulk magnetic penetration depth and the coherence length reported for this high κ material are, respectively, $\lambda(T=0)\approx 106-230$ nm (Refs. 14 and 15) and $\xi(T=0)\approx 3.8-6.8$ nm.[14,16] Contrary to layered materials such as 2H-$NbSe_2$, it is a hard but brittle material. Its cubic structure allows one to bring the tip very close to the surface, in order to reduce R_N, without damaging the sample surface or the tip. On the other hand, this material cannot be cleaved and hence requires a careful surface preparation. This explains why this "old" superconductor has only rarely been studied by STM. To our knowledge, the only STM study in V_3Si concerns the hexagonal-to-square vortex lattice transition.[17]

The samples were prepared from (001) and (111) small single crystals of V_3Si ($\sim 2\times 2\times 0.5$ mm^3) characterized by a sharp SC transition at $T_c=17$ K, as measured by superconducting quantum interference device (SQUID) magnetometry. They were mechanically polished using a 1 μm diamond powder and annealed at 600 °C under UHV for 1 h. To remove a damaged surface layer, the samples were chemically etched which yielded a bright metallic surface.[18] In order to best avoid the oxidation of the V_3Si surface after etching, the samples were immersed in pure ethanol and loaded wet into the fast load-lock UHV chamber of the STM.

Figure 1 gives an example of the tunneling characteristics of such V_3Si-MgB_2 tunneling junctions. Panel (a) shows a typical dI/dV tunneling spectrum obtained in the QP tunneling regime. Two pairs of peaks are found to be at $\Delta_1=\pm 5.7$ meV and $\Delta_2=\pm 10.2$ meV [see red and blue arrows, respectively, in Fig. 1, panel (a)]. Considering a superconductor-insulator-superconductor (SIS) junction with a two-gap SC on one side, these peaks can be attributed to $\Delta_1=\Delta^{\pi}_{MgB_2}+\Delta_{V_3Si}$ and $\Delta_2=\Delta^{\sigma}_{MgB_2}+\Delta_{V_3Si}$. Taking for MgB_2 (Ref. 19) $\Delta^{\pi}_{MgB_2}=2.8$ meV and $\Delta^{\sigma}_{MgB_2}=7.4$ meV, one obtains a rough but still reasonable estimate for the SC gap of V_3Si $\Delta_{V_3Si}=2.8\pm 0.2$ meV. In panel (b) we focus on the low energy part of the spectra and show their evolution as the SC tip is brought closer and closer to the sample surface. When the tunneling resistance becomes of the order of 2×10^5 Ω or lower, an additional peak appears at zero bias. The amplitude of the peak increases significantly when the tunneling resistance and/or the temperature is lowered. Thus, this peak cannot be interpreted as the thermal one seen conventionally in SC-SC junctions at Δ_1-Δ_2 since the latter is independent of the tunneling resistance and has an opposite temperature dependence.

To prove that the observed effect is due to the Josephson tunneling, we have followed Dynes *et al.*[6] and compared the height of the peak to the prediction of a model in the fluctuation regime.[8] To achieve this, each $I(V)$ spectrum was fitted around zero bias using the following formula:

$$I(V)=A\frac{V}{V^2+V_p^2}, \tag{1}$$

where A and V_p are the two fitting parameters of the model which predicts a linear dependence on the variation in $\sqrt{4e^2A/\hbar V_p}$ as a function of $1/R_N$. This linear dependence is clearly found in the experimental data presented in Fig. 1(c).

The vortex imaging was achieved in a magnetic field of 1.15 T. Two complete conductance maps were measured: one in the QP regime, at $R_N=6.25$ MΩ, where the contribution of the Cooper pairs in the tunneling current is negligible, and the other, at $R_N=60$ kΩ, corresponding to the Josephson regime. In order to avoid tip crashes, a special mapping mode was developed: the tip scans the surface at $R_N^{\mathrm{scan}}\approx 10^6-10^9$ Ω as in an ordinary STM. At each map point the scan is interrupted and the tip is made to approach a higher current set point; the spectroscopy curve $I(V)$ is acquired at this tunneling resistance; and the tip is then retracted back to the scan position prior to moving to the next map point.[9]

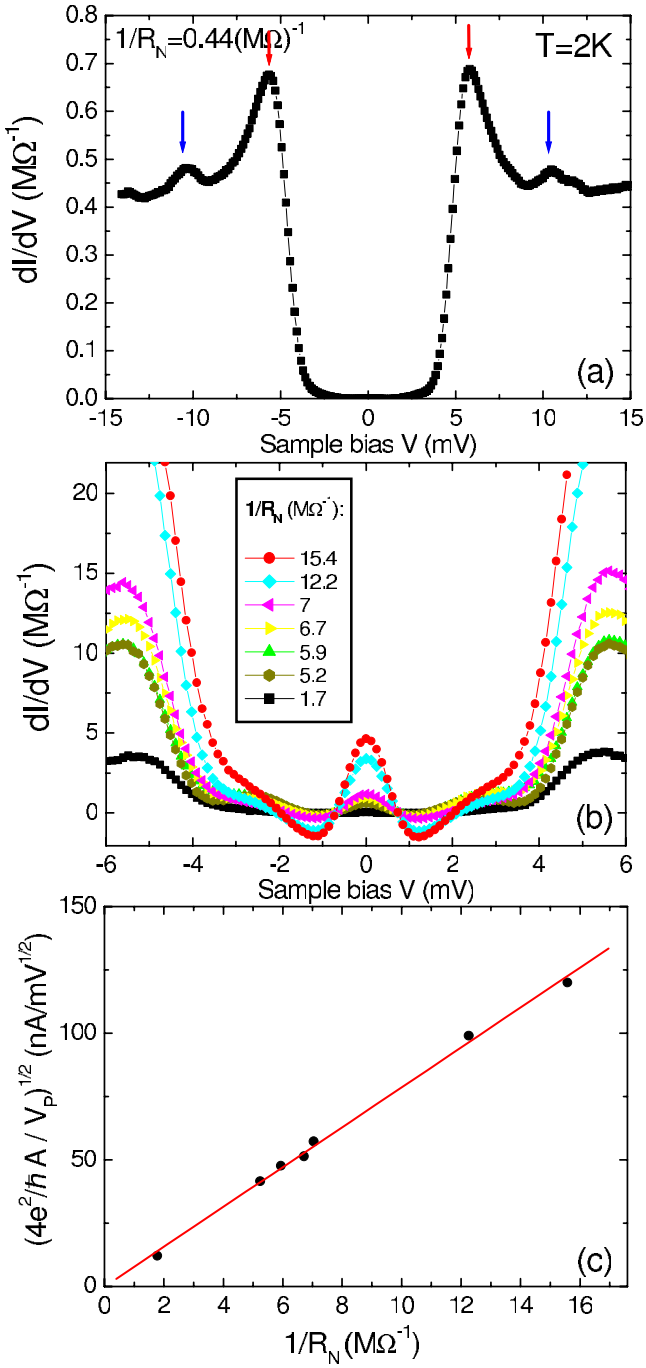

FIG. 1. (Color online) SC-SC tunneling spectra at various tip-sample distances. In panel (a): the tunneling conductance spectrum (points) measured at $R_N=2.27$ MΩ. At this condition, only the QP tunneling occurs. In panel (b): as the tip-sample distance is diminished the JC appears as a zero-bias peak in the conductance curve. Panel (c): the height of the JC peak (dots) was fitted using the model (Ref. 8) (line). The ratio $(4e^2\hbar A/V_p)^{1/2}$ was plotted as a function of the inverse normal resistance $1/R_N$.

Figure 2(a) presents a zero-bias conductance map obtained in the QP regime. The image reveals the hexagonal vortex lattice with the unit-cell parameter $a=56$ nm.[20] In the Josephson regime, zero-bias conductance maps also reveal the vortices [Fig. 2(b)]. These maps, however, are more com-

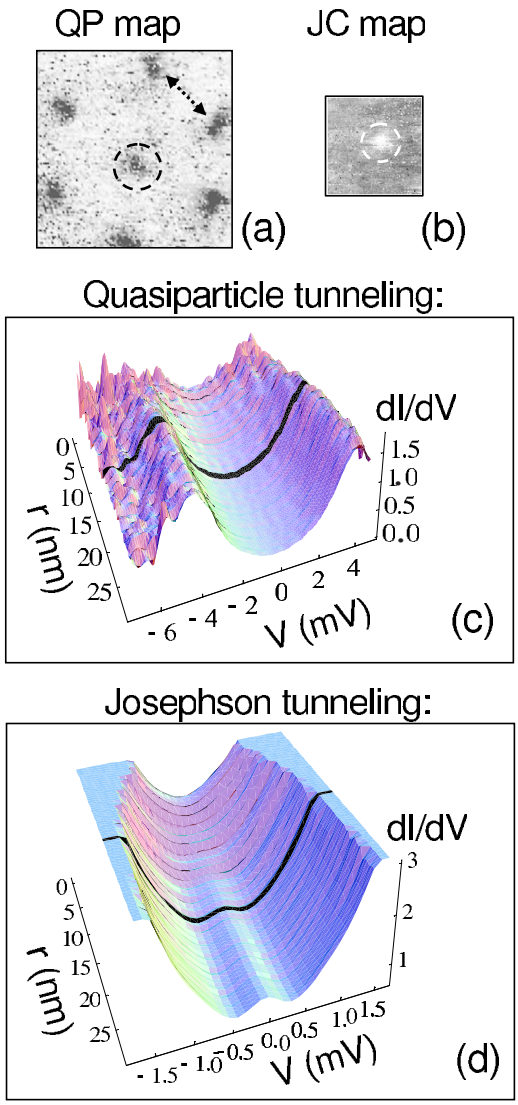

FIG. 2. (Color online) Panel (a): a 125×125 nm^2 zero-bias conductance map obtained in QP configuration ($B=1.15$ T) reveals triangular vortex lattice. Panel (b): a 8×8 nm^2 vortex map in Josephson regime. Panels (c) and (d) are 3D plots of the tunneling conductance as a function of distance r from the vortex center for QP and Josephson regimes, respectively. The spectra are normalized to dI/dV 8 mV in (c), and to dI/dV 4 mV in (d). The black lines in (c) and (d) are examples of the spectra obtained by averaging over the dashed circles in panels (a) and (b), respectively.

plex to analyze since the zero-bias conductance in the JC regime depends on both QP and JC contributions. Far from the vortex cores, the SC gap in the QP spectrum is fully opened and the QP contribution into the zero-bias conductance is small [Fig. 2(c)]. At the same time, the JC peak has its maximum value and, thus, dominates the total signal at zero bias [Fig. 2(d)]. Toward the vortex core, however, the situation changes dramatically: the number of states in the QP spectrum rapidly increases due to gap filling and closing [Fig. 2(c)], and the JC peak disappears [Fig. 2(d)]. Finally, inside the vortex core, the tunneling conductance at zero bias is dominated by the QP term.

As it has been recently shown,[21] the conductance maps

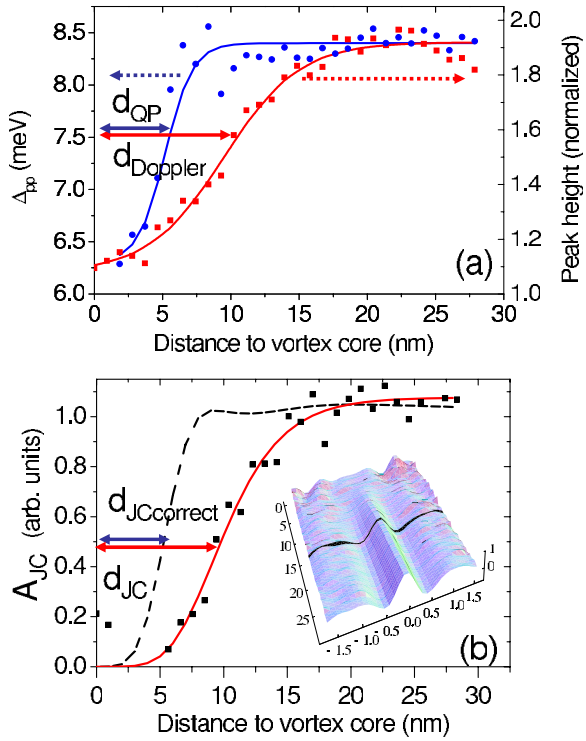

FIG. 3. (Color online) In panel (a), we plot the peak-to-peak distance and the peak height shown in QP tunneling. Using these curves, we find the vortex size seen in the QP tunneling to be $d_{QP}=5$ nm and the Doppler length $d_{Doppler}=12$ nm. Panel (b): Josephson peak amplitude A_{JC} as a function of r. It vanishes over a characteristic distance of $d_{JC}=10$ nm. Solid line—a polynomial fit curve; dashed line: the same curve but recalculated using corrected values for R_N: $A_{JCcorrect}(r)$. Inset: 3D plot of the JC peak after subtraction of the background.

acquired with a SC tip in the QP regime contain information about both the coherence length ξ and the penetration depth λ. Indeed, toward the vortex core, the SC order parameter (and, consequently, the SC gap in the QP spectrum) vanishes on the scale of ξ.[1] Far from the vortex cores, however, the excitation spectrum is slightly affected by the local screening currents through the Doppler effect.[21] This allows one to map the supercurrents surrounding vortices and extraction of λ.

It is interesting to compare quantitatively the spatial evolution of the JC peak A_{JC} near the vortex to the variations in the QP spectra. As it has been recently shown, the variation in the QP peak height gives an additional length $d_{Doppler}$ which is related to the screening currents. Experimentally, one observes the decrease in the distance separating QP peaks and the gap filling over the scale d_{QP} [Fig. 2(c)]. Far from the vortex cores, however, the main observable effect is a decrease in the QP peak height over the scale $d_{Doppler}\sim\lambda$ due to the Doppler shift.[21] In Fig. 3 we plot the QP peak-to-peak separation Δ_{pp}, the QP peak height, and the JC peak amplitude A_{JC} as a function of distance from the vortex center r. In order to substantially improve the signal-to-noise ratio, the conductance spectra were azimuthally averaged over circles centered on the vortex core [dashed circles in Figs. 2(a) and 2(b)]. Note that such an averaging makes sense only for small r as it washes out angular features in the

vortex lattice. All plotted curves manifest a very similar behavior: low values in the vortex cores, then a rise, and, finally, saturation at large distances. Thus, the simplest way to characterize each of them is to estimate the distance corresponding to the half amplitude of the total variation. The two curves in Fig. 3(a) clearly evolve on two different scales: $d_{QP}=5$ nm for the peak-to-peak separation energy and about $d_{Doppler}=10$ nm for peak height variation. The first one is clearly associated with ξ of V_3Si.[14,16] The second one characterizes the spatial variation in the intensity of screening currents.[21]

At first glance, the dynamics of d_{JC} [Fig. 3(b)] takes place on the same scale as the Doppler effect $d_{JC} \approx d_{Doppler}$. At this point, a particular feature of our JSTM experiment must be taken into account. In fact, in order to avoid the preamplifier saturation, the regulation bias was chosen inside the SC gap. As a result, the tip-to-sample distance, and therefore the real R_N, was not kept constant but continuously increased approaching the vortex core. Since in the fluctuation regime the JC peak amplitude varies as $1/R_N^2$,[8] the variations $R_N(r)$ lead to an additional reduction in A_{JC} when approaching the vortex core. To correct A_{JC} we proceeded as follows: (i) The ratio Ratio(r) between dI/dV (2.5 mV) in the QP regime [Fig. 2(c)] and in the Josephson regime [Fig. 2(d)] was extracted. Note that at this bias, the Josephson term in the tunneling conductance is negligible in both regimes and the signal is dominated by QPs. Since R_N in the QP regime was kept constant (the regulation bias was taken well beyond the gap energies), the variation Ratio(r) reflects the spatial evolution of R_N in the Josephson regime. (ii) The corrected value for the amplitude of the JC peak was evaluated as $A_{JCcorrect} = A_{JC} \times \text{Ratio}(r)^2$. The $A_{JCcorrect}(r)$ is presented as a dashed line in Fig. 3(b). Its characteristic scale $d_{JCcorrect} \approx 5$ nm is very close to $d_{QP} \sim \xi$. This could suggest the JC peak to be insensitive to the intensity of local supercurrents. Note, however, that $A_{JCcorrect}$ is obtained using the model[8] where validity near the vortex is unclear.

In conclusion, we have reported a Josephson STM experiment of the conventional superconductor V_3Si. It was first shown that the JC amplitude follows the Josephson fluctuation regime. The vortex lattice was used as the simplest situation where the SC order parameter varies spatially. The JC vanishes when entering the vortex over a characteristic distance of $\sim 5-10$ nm. This distance is found to be very close to the vortex size seen in the QP tunneling spectra. It would be interesting to substantiate our conclusions with both theoretical insight, by the consideration of the fluctuating JC near a vortex, and future JSTM experiments on such systems.

The authors wish to thank Abbay Shukla (IMPMC, Paris, France) and Alfred Manuel (DPMC, University of Geneva, Switzerland) for the generous loan of the V_3Si samples, Michelle Jacquet and Melanie Escudier (INSP, Paris, France) for skilled assistance, and Frederic Bernardot (INSP, Paris, France) for SQUID measurements.

*yves.noat@insp.jussieu.fr

[1] H. F. Hess, R. B. Robinson, and J. V. Waszczak, Phys. Rev. Lett. **64**, 2711 (1990).
[2] Ø. Fischer, M. Kugler, I. Maggio-Aprile, C. Berthod, and C. Renner, Rev. Mod. Phys. **79**, 353 (2007).
[3] Ch. Renner, B. Revaz, K. Kadowaki, I. Maggio-Aprile, and Ø. Fischer, Phys. Rev. Lett. **80**, 3606 (1998).
[4] J. Smakov, I. Martin, and A. V. Balatsky, Phys. Rev. B **64**, 212506 (2001).
[5] B. D. Josephson, Phys. Lett. **1**, 251 (1962).
[6] O. Naaman, W. Teizer, and R. C. Dynes, Phys. Rev. Lett. **87**, 097004 (2001); O. Naaman, R. C. Dynes, and E. Bucher, Int. J. Mod. Phys. B **17**, 3569 (2003).
[7] J. Rodrigo, H. Suderow, and S. Vieira, Eur. Phys. J. B **40**, 483 (2004).
[8] M. Ivanchenko and L. A. Zil'berman, Zh. Eksp. Teor. Fiz. **55**, 2395 (1968) [Sov. Phys. JETP **28**, 1272 (1969)].
[9] Th. Proslier, A. Kohen, Y. Noat, T. Cren, D. Roditchev, and W. Sacks, Europhys. Lett. **73**, 962 (2006).
[10] F. Giubileo, D. Roditchev, W. Sacks, R. Lamy, D. X. Thanh, J. Klein, S. Miraglia, D. Fruchart, J. Marcus, and P. Monod, Phys. Rev. Lett. **87**, 177008 (2001).
[11] Y. Wang, T. Plackowski, and A. Junod, Physica C **355**, 179 (2001); P. Szabó, P. Samuely, J. Kacmarcik, T. Klein, J. Marcus, D. Fruchart, S. Miraglia, C. Marcenat, and A. G. M. Jansen, Phys. Rev. Lett. **87**, 137005 (2001).
[12] G. F. Hardy and J. K. Hulm, Phys. Rev. **89**, 884 (1953).
[13] D. F. Moore, R. B. Zubeck, J. M. Rowell, and M. R. Beasley, Phys. Rev. B **20**, 2721 (1979).
[14] D. K. Christen, H. R. Kerchner, S. T. Sekula, and Y. K. Chang, Physica B & C **135**, 369 (1985).
[15] T. J. Greytak and J. H. Wernick, J. Phys. Chem. Solids **25**, 535 (1964).
[16] M. Yethiraj, D. K. Christen, D. McK. Paul, P. Miranovic, and J. R. Thompson, Phys. Rev. Lett. **82**, 5112 (1999).
[17] C. E. Sosolik, J. A. Stroscio, M. D. Stiles, E. W. Hudson, S. R. Blankenship, A. P. Fein, and R. J. Celotta, Phys. Rev. B **68**, 140503(R) (2003).
[18] J. B. Hastings, Y. Fujii, G. Shirane, and S. J. Williamson, Phys. Rev. B **28**, 322 (1983).
[19] H. Schmidt, J. F. Zasadzinski, K. E. Gray, and D. G. Hinks, Physica C **385**, 221 (2003).
[20] The value $a=56$ nm corresponds to the local magnetic field of 0.77T, lower than the external one (1.15T). We attribute it to the fact that the field penetrates preferentially in dislocations and grain boundaries which may be a result of the sample preparation.
[21] A. Kohen, Th. Proslier, T. Cren, Y. Noat, W. Sacks, H. Berger, and D. Roditchev, Phys. Rev. Lett. **97**, 027001 (2006).